Determination of resonance spectra for bound chaotic systems

1994 J. Phys. A: Math. Gen. 27 763

(http://iopscience.iop.org/0305-4470/27/3/020)

J. Phys. A: Math. Gen. 27 (1994) 763–785. Printed in the UK

Determination of resonance spectra for bound chaotic systems

Per Dahlqvist
Mechanics Department, Royal Institute of Technology, S-100 44 Stockholm, Sweden

Received 18 August 1993, in final form 1 November 1993

Abstract. We consider the computation of the eigenvalues of the evolution operator—*the resonance spectrum*—by means of the zeros of a *zeta function*. In particular we address the problems of applying this formalism to bound chaotic systems, caused by e.g. intermittency and non-completeness of the symbolic dynamics. For bound intermittent system we derive an approximation of the zeta function. With the aid of this zeta function it is argued that bound systems with *long time tails* have branch cuts in the zeta function and traces (of the evolution operator) approaching unity as a power law. We also show that the dominant time scale can be much longer than the period of the shortest periodic orbit, as is, for example, the case for the hyperbola billiard. Isolated zeros of the zeta function for the hyperbola billiard are evaluated by means of a cycle expansion. Crucial for the success of this approach is the identification of a sequence of periodic orbit responsible for a logarithmic branch cut in the zeta function. Semiclassical implications are briefly discussed.

1. Introduction

Time correlations provide an efficient tool for the analysis of dynamical systems. For some chaotic systems correlations decay exponentially, reflecting loss of memory during evolution. Often the correlation function is found to be modulated by some typical frequencies related to the periodic orbits of the system. Its Fourier transform will thus have poles (*resonances*) in the complex frequency k plane. The imaginary parts correspond to the decay rates and the real parts to the oscillation frequencies. Integrable systems have resonances *on* the real axis, reflecting quasiperiodicity of the motion.

A rigorous theory for resonances has so far been developed only for Axiom-A systems [1–4]. The correlation function is then meromorphic (i.e. it has nothing worse than poles) in a strip around the real k-axis. For mixing Axiom-A maps one can establish exponential bounds on the decay of correlations, i.e. there is a strip (gap) above the real axis without resonances. But even for Axiom-A flows the resonances may lie arbitrarily close to the real axis leading to non-exponential decay of correlations [5, 6]. It is a general experience that the positions of the resonances are independent of the particular observables whereas the residues are not. This is proven only for Axiom-A systems but numerical work suggests that it holds more generally. This is very intriguing since one can thus characterize a system by its (classical) resonance spectrum, in nice analogy with its quantum spectrum.

However, Axiom-A systems are very idealistic systems from a physical point of view, although they may be realized by, for example, some open scattering systems. The purpose of the present paper is to study resonance spectra in *bound* Hamiltonian systems, exhibiting chaos. Then we know that there is a trivial pole at $k = 0$ reflecting the boundedness of the system. All other resonances lie in the upper halfplane. This is essentially all we know for certain.

0305-4470/94/030763+23$07.50

Crucial for the successful theory of Axiom-A system is the existence of a finite Markov partition. One can thus perform a well converging cycle expansion of a zeta function in order to locate the resonances [4]. Such finite grammar does generally not exist for bound systems. This leaves us without any *a priori* knowledge of the analytical structure of the zeta function we are going to study.

We will restrict ourselves to ergodic billiards in the Euclidean plane, thus avoiding the presence of stability islands which seems impossible to avoid in smooth potentials [7]. Seemingly all systems of this type have one thing in common; they are intermittent. Typically, the motion will intermittently alternate between a chaotic region of phase space and a regular one. This might imply power law decay of correlations. In a paper by Baladi, Eckmann and Ruelle [8] (hereafter referred to as the BER approximation) it is demonstrated how the approximate positions of the resonances for intermittent systems may be calculated. This result is directly applicable to a wide class of bound chaotic systems and we will make use of this observation in the following.

The second main theme of the paper is a periodic orbit sum rule discovered in [9]. It is thus shown that a certain weighted sum over all periodic orbits (which turn out to be identical to the trace of the evolution operator) tends to unity as $t \to \infty$. This is an asymptotic result and it is of course highly interesting to know how this asymptotic limit is approached. This periodic orbit sum is a crucial ingredient when computing correlations in quantum spectra.

The paper is outlined as follows. We begin, in section 2.1, by reviewing the derivation of the classical zeta function whose zeros are associated with the resonances. Then, in section 2.2, we review how, according to the BER approximation, the positions of the resonances are related to a simple probability distribution associated with the system. In section 3 we relate, by heuristic arguments, different features of this probability distribution to the resonance spectrum. In section 4 we apply cycle expansions of the zeta function to a specific dynamical system—the hyperbola billiard. Section 3 and 4 run along rather separate lines with only occasional cross references. In section 5 we discuss the relevance of our result for correlations in quantum spectra.

2. Theory

2.1. The zeta function

Periodic orbit expansions (or cycle expansions—we will use the words cycles, periodic orbits or simply orbits synonymously in the following) of *zeta functions* have proved to be successful for calculating various averages of chaotic sets. Most of the labour has so far been devoted to maps, that is, systems with discrete time. A zeta function for systems with continuous time has been derived in [10]. We briefly review the derivation. The resonances k_n may formally be associated with the eigenvalues $\exp(ik_n t)$ of the evolution operator $\mathrm{tr}\mathcal{L}^t$, acting on a function $\Phi(x)$ as

$$\mathrm{tr}\,\mathcal{L}^t\Phi(x) = \int \delta(x - f^t(y))\Phi(y)\,\mathrm{d}y. \tag{1}$$

The phase-space point x is taken by the flow to $f^t(x)$ during time t. The structure, $\exp(ik_n)^t$, of the eigenvalues is required by the semigroup property of the operator: $\mathcal{L}^{t_1+t_2} = \mathcal{L}^{t_1}\mathcal{L}^{t_2}$. Our main concern in this paper is to compute the trace of this operator,

that is, the sum of its eigenvalues. The trace may be written as a sum over the isolated periodic orbits in the system.

$$\operatorname{tr}\mathcal{L}^t = \int \delta(x - f^t(x))\,\mathrm{d}x = \sum_p T_p \sum_{n=1}^{\infty} \frac{\delta(t - nT_p)}{|\det(1 - M_p^n)|} \tag{2}$$

where n is the number of repetitions of primitive orbit p, having period T_p and M_p is the Jacobian of the Poincaré map.

The function $\operatorname{tr}\mathcal{L}^t$, (we will refer to this object as simply the *trace* in the following) may be written as the Fourier transform of the logarithmic derivative of a *zeta function*:

$$\operatorname{tr}\mathcal{L}^t = \frac{1}{2\pi\mathrm{i}} \int_{-\infty}^{\infty} \mathrm{e}^{\mathrm{i}kt} \frac{Z'(k)}{Z(k)}\,\mathrm{d}k. \tag{3}$$

We restrict ourselves to systems with two degrees of freedom for which all periodic orbits are isolated and unstable. The zeta function then reads

$$Z(k) = \prod_p \prod_{m=0}^{\infty} \left(1 - \frac{\mathrm{e}^{-\mathrm{i}kT_p}}{|\Lambda_p|\Lambda_p^m}\right)^{m+1} \tag{4}$$

where Λ_p is the expanding eigenvalue of M_p. Each zero k_α of $Z(k)$ induces a pole in the integrand and is identified with an eigenvalue of the evolution operator. The leading zero is the escape rate, which is zero for a bound system; $k_0 = 0$.

If the zeta function is entire we can write

$$\operatorname{tr}\mathcal{L}^t = 1 + \sum_{\alpha \neq 0} \mathrm{e}^{\mathrm{i}k_\alpha t}. \tag{5}$$

If there is a gap between the real axis and the non-trivial zeros then the trace approach unity exponentially fast.

The corresponding zeta function for systems with a hyperbolic analytic Poincaré map has been shown to be entire provided the existence of a finite Markov partition [4]. These conditions generally break down for bound systems.

However, the trace is expected to converge towards unity for bound systems, under quite general circumstances, as was shown in [9]. This is often referred to as a periodic orbit sum rule.

In equation (5) we have neglected the integral along the upper semicircle. It may be argued that this can only yield a deltafunction $\delta(t)$ and derivatives of the deltafunction $\delta^n(t)$.

As an example consider the following simplified Axiom-A system (it may be realized by a three disk scatterer with the disks infinitely separated). We take the system to have a binary complete symbolic dynamics. An orbit p has eigenvalue $\Lambda_p = \Lambda_0^{n_p}$ and period $T_p = n_p T_0$ where n_p is the length of the symbol code p. Expanding the product over cycles gives, cf [11]

$$Z(k) = \prod_{m=0}^{\infty} \left(1 - 2\frac{\mathrm{e}^{-\mathrm{i}kT_0}}{\Lambda_0^{m+1}}\right)^{m+1}. \tag{6}$$

The product is convergent so we can just read of the zeros

$$k_{n,m} = \frac{1}{T_0}(2\pi n + \mathrm{i}[(m+1)\ln\Lambda_0 - \ln 2]) \qquad n = 0, \pm 1, \pm 2, \ldots. \tag{7}$$

The spacing between zeros in the real direction is directly related to the single timescale in the system—the period of the shortest periodic orbit. The situation for bound systems is generally much more complicated, as we will see later; they may exhibit an infinite set of time scales.

For a more general system with complete binary grammar the spectrum above will give the gross structure, whereas longer periodic orbit provide corrections [11, 12]. However, even for small deviations from the simple example above there will be quite intricate cancellations between poles and zeros [4, 11, 13] of the individual m-factors.

For bound systems there is generally, as we said, no finite Markov partition and no hyperbolicity. In this paper we will study the zeta function (4) for the first time for a non-hyperbolic flow. We have then no reason to expect entireness of the zeta function and we will concentrate on revealing the main singularities. Note that a singularity, such as a pole, in the zeta function cannot be interpreted as an eigenvalue of the evolution operator. We will not touch upon the difficult question of how to compute correlation function in this case, but rather concentrate on the analytic structure (zeros, poles branch cuts ...) of the zeta function and the behaviour of the corresponding trace, as defined by equation (2).

2.2. *The BER approximation—a probabilistic approach*

In [8] a method has been given for the determination of the approximate resonance spectrum for intermittent systems. In such a system there are two, more or less, distinct phases; one regular and one irregular (chaotic). Call the consecutive instants when the system enters the regular phase $\{t_i\}$ and consider the intervals $I_i = [t_{i-1}, t_i]$. Provided the chaotic phase is *chaotic enough*, the motions in different intervals are nearly mutually independent. In particular the lengths of these intervals $\Delta_i = t_i - t_{i-1}$ are mutually independent and Δ may be considered as a stochastic variable with probability distribution $p(\Delta)$. Consider now the Fourier transform

$$\tilde{p}(k) = \int_0^\infty \mathrm{e}^{-\mathrm{i}k\Delta} p(\Delta)\,\mathrm{d}\Delta. \tag{8}$$

Under the assumption above, the roots of

$$1 - \tilde{p}(k) = 0 \tag{9}$$

will now provide the approximate resonances, that is, the approximate zeros of the zeta function.

Reference [8] does not discuss zeta functions. However, having two functions $Z(k)$ and $1 - \tilde{p}(k)$ with approximately the same zeros (both have also the trivial zero $k_0 = 0$ in common) we immediately suspect them to be closely related. Indeed, we will show that $Z(k) \approx 1 - \tilde{p}(k)$ in the BER approximation. To this end we will modify the calculation of [8] so as to apply directly to the trace of the evolution operator.

First we turn the phase-space integral in equation (2) into a time average:

$$\mathrm{tr}\,\mathcal{L}^t = V\langle\delta(x(t_0) - x(t_0 + t))\rangle_{t_0} \tag{10}$$

where V is the available phase-space volume.

Let now $\mathrm{tr}_m(t)$ be the trace conditioned by 'if $t_0 \in I_n$ then $t + t_0 \in I_{n+m}$'. The trace is now expressed as the sum $\mathrm{tr}\mathcal{L}^t = \sum_{m=0} \mathrm{tr}_m(t)$. We now define two probability distributions:

• $f_1(x, u)$ is the probability that the system is at phase-space point x at time t_0 and that there is time u left of the current interval.

• $f_2(y, v)$ is the probability that the system is at point y at time $t_0 + t$ and that time v has elapsed since the current interval was entered.

We can now express the average as

$$\mathrm{tr}_m(t) \approx V\langle\Delta\rangle \int \mathrm{d}u\,\mathrm{d}v\, p^{*(m-1)}(t-u-v) \int \mathrm{d}x\,\mathrm{d}y\,\delta(x-y) f_1(x,u) f_2(y,v) \tag{11}$$

where $p^{*n}(t)$ is the n-fold convolution of $p(t)$, and $\langle\Delta\rangle$ the mean length of the intervals. We now express the convolution by means of the Fourier transforms

$$\begin{aligned}\mathrm{tr}_m(t) &\approx \frac{V\langle\Delta\rangle}{2\pi} \int \mathrm{d}k\, \mathrm{e}^{\mathrm{i}kt} \tilde{p}(k)^{m-1} \int \mathrm{d}u\,\mathrm{d}v\,\mathrm{d}x\,\mathrm{d}y\,\delta(x-y)\mathrm{e}^{-\mathrm{i}ku} f_1(x,u)\mathrm{e}^{-\mathrm{i}kv} f_2(y,v) \\ &= \frac{V\langle\Delta\rangle}{2\pi} \int \mathrm{d}k\, \mathrm{e}^{\mathrm{i}kt} \tilde{p}(k)^{m-1} \int \mathrm{d}x\, \tilde{f}_1(x,k)\tilde{f}_2(x,k). \end{aligned} \tag{12}$$

We can now sum over m and arrive at

$$\mathrm{tr}\,\mathcal{L}^t \approx \mathrm{tr}_0(t) + \frac{V\langle\Delta\rangle}{2\pi} \int \mathrm{d}k\, \mathrm{e}^{\mathrm{i}kt} \frac{1}{1-\tilde{p}(k)} \int \mathrm{d}x\, \tilde{f}_1(x,k)\tilde{f}_2(x,k). \tag{13}$$

Comparing with equation (3), and neglecting tr_0, we identify

$$\frac{Z'(k)}{Z(k)} \approx \frac{V\langle\Delta\rangle\mathrm{i}}{1-\tilde{p}(k)} \int \mathrm{d}x\, \tilde{f}_1(x,k)\tilde{f}_2(x,k). \tag{14}$$

Moreover, we can identify:

$$Z(k) \approx \hat{Z}(k) \equiv 1 - \tilde{p}(k) \tag{15}$$

provided that

$$V\langle\Delta\rangle \int \mathrm{d}x\, \tilde{f}_1(x,k)\tilde{f}_2(x,k) = \int \Delta \mathrm{e}^{-\mathrm{i}k\Delta} p(\Delta)\,\mathrm{d}\Delta. \tag{16}$$

To verify that this is indeed the case we make use of the fact the remaining time of the current interval u is a function of the phase-space point $u = g_1(x)$ so that

$$f_1(x,u) = \phi(x)\delta(u - g_1(x)) \tag{17}$$

where $\phi(x)$ is the phase-space density. Similarly we have

$$f_2(x,v) = \phi(x)\delta(v - g_2(x)). \tag{18}$$

We can now express the probability function $p(\Delta)$ weighted with the length of the interval Δ in terms of g_1 and g_2

$$\Delta \cdot p(\Delta) = \langle\Delta\rangle \int \phi(x)\delta(\Delta - g_1(x) - g_2(x))\,\mathrm{d}x. \tag{19}$$

Also, using the fact that the phase density is uniform, $\phi(x) \cdot V = 1$, equation (16) is easily verified.

In this section we have been able to give the zeta function a probabilistic interpretation and have constructed an approximate zeta function $\hat{Z}(k)$ whose zeros should be interpreted as the approximate resonances. This is one of the main achievements of the paper. To establish this correspondence we have neglected the function $\mathrm{tr}_0(t)$ describing correlations within an interval. These correlations are thus inherent in $Z(k)$ but not in $\hat{Z}(k)$. We therefore expect deviations in the results obtained from the two functions for small t.

3. Phenomenology of the BER approximation

The close relationship between $Z(k)$ and $\hat{Z}(k)$ as defined by equation (15) motivates a study of how different features of the probability function $p(\Delta)$ affects the spectrum and trace of the evolution operator. Throughout this section we will ignore the difference between $Z(k)$ and $\hat{Z}(k)$, that is we will temporarily assume that $Z(k) = \hat{Z}(k)$. The reader should keep in mind that the spectra and traces obtained here are of course only approximations of those of real dynamical systems and the errors are not under control.

We begin by studying a model (model A) with a sharp step and exponential decay

$$p_{\mathrm{A}}(\Delta) = \begin{cases} 0 & \Delta < T_1 \\ N\mathrm{e}^{-\Delta/T_2} & \Delta \geqslant T_1 \end{cases} \tag{20}$$

where N is a normalization factor. We take the Fourier transform and get

$$Z_{\mathrm{A}}(k) = \frac{\mathrm{e}^{-\mathrm{i}kT_1}}{1+\mathrm{i}kT_2} - 1. \tag{21}$$

One can obtain the following asymptotic expression for the zeros of this function

$$k_n \approx \frac{1}{T_1}\left(\pm 2\pi(n-\tfrac{1}{4}) + \mathrm{i}\ln\left(\frac{T_2}{T_1}2\pi(n-\tfrac{1}{4})\right)\right) \qquad n+1,2,3,\ldots \tag{22}$$

which agrees very well for large n and/or large T_2/T_1 (cf figure 1(*a*)). We see that the relevant time scale is T_1, whereas T_2 is of minor significance. $Z_{\mathrm{A}}(k)$ has a simple pole at $k + \mathrm{i}/T_2$ reflecting the behaviour of $p_{\mathrm{A}}(\Delta)$ at infinity. This is all we need to calculate the trace by means of equation (3). We get

$$\mathrm{tr}\,\mathcal{L}^t = \Psi_{\mathrm{zeros}}(t) + \Psi_{\mathrm{tail}}(t) \tag{23}$$

where

$$\Psi_{\mathrm{zeros}}(t) = 1 + \sum_n \mathrm{e}^{\mathrm{i}k_n t} \approx 1 + \left(\frac{T_2}{T_1}\right)^{-t/T_1} \sum_{n=1}^{\infty} 2\cos\left(2\pi(n-\tfrac{1}{4})\frac{t}{T_1}\right)(2\pi(n-\tfrac{1}{4}))^{-t/T_1} \tag{24}$$

and

$$\Psi_{\mathrm{tail}}(t) = -\mathrm{e}^{-t/T_2}. \tag{25}$$

The sum (24) is absolutely convergent when $t/T_1 > 1$ and tends exponentially to unity as $t/T_1 \to \infty$. To study its behaviour for small t/T_1 we have to smear the function term by term, that is convolute it with a Gaussian having width σ. For a general spectrum $k_n = \pm a_n + \mathrm{i}b_n$ we find for the smeared sum

$$\Psi_{\mathrm{zeros},\sigma}(t) = 2\sum_n \exp\left(-\frac{\sigma^2}{2}(a_n^2 - b_n^2) - b_n t\right)\cos(a_n t - \sigma^2 a_n b_n). \tag{26}$$

For all relevant spectra this sum is absolutely convergent for any smearing width σ.

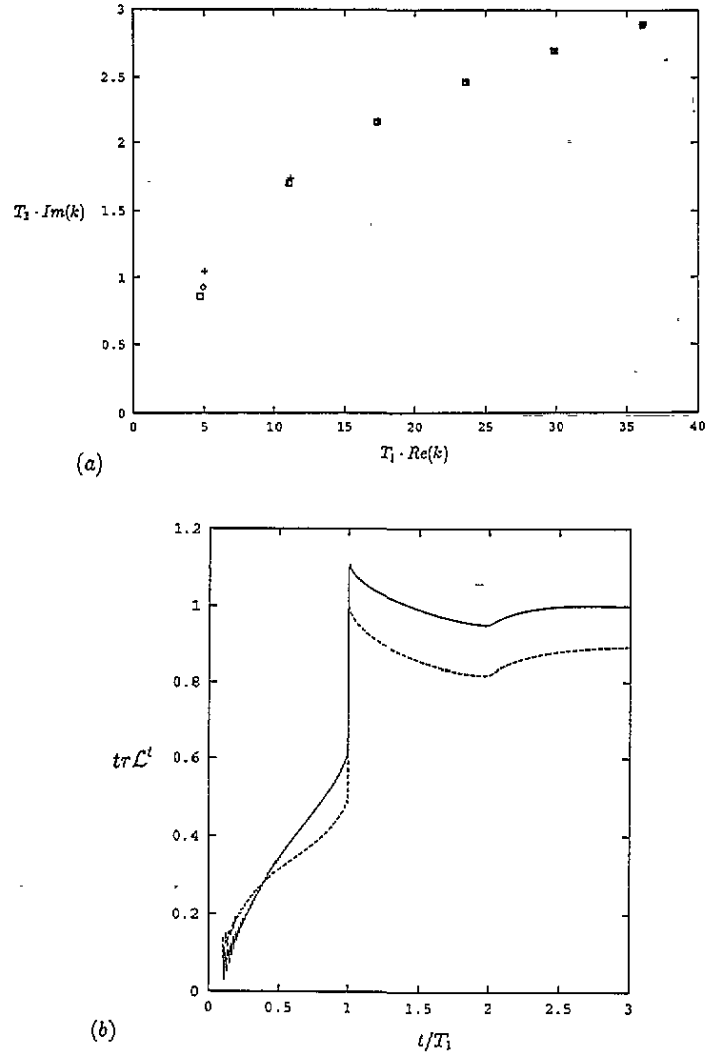

Figure 1. The spectrum (*a*) of model A (◇) and B (+) and its asymptotic expression (□) and (*b*) the trace for model A (full line) and B (dashed). The asymptotic expression has been used to calculate its discrete contribution Ψ_{zeros} to the trace.

The trace when $T_2/T_1 = 0.5$, is plotted in figure 1(*b*). The sharp step at $t/T_1 = 1$ reflects the sharp step in $p_A(\Delta)$. They are indeed steps whenever t/T_1 is an integer, but due to the exponential damping they are less pronounced.

Let us now consider a case with power-law decay of $p(\Delta)$ (model B).

$$p_B(\Delta) = \begin{cases} 0 & \Delta < T_1 \\ N(T_1/\Delta)^m & \Delta \geqslant T_1. \end{cases} \tag{27}$$

Again we compute the Fourier transform and seek the zeros of

$$Z_B(k) = (m-1)E_m(ikT_1) - 1 \tag{28}$$

where $E_m(z)$ is the exponential integral. It turns out that all zeros are positioned where we can use the asymptotic expansion of $E_m(z)$, see [14]. The positions of the zeros are well

approximated by

$$k_n \approx \frac{1}{T_1}\left(\pm 2\pi(n-\tfrac{1}{4}) + \mathrm{i}\ln\left(\frac{2\pi(n-1/4)}{m-1}\right)\right) \qquad n = 1, 2, 3, \ldots \tag{29}$$

which is equivalent with *model A* when $m - 1 = T_1/T_2$, that is when the height of the step in $p(\Delta)$ is the same. High zeros (large n) are thus only sensitive to the immediate vicinity of the step. In figure 1(a) the exact zeros of models A and B are compared with this asymptotic result. Formally, if we increase m(or T_1/T_2 in model A) $p_B(\Delta)$ will tend to a delta peak, and the resonances approach the real axis, resembling an integrable system. Of course the assumption in the BER approximation is then no longer fulfilled.

However there is one major difference to model A. The zeta function is no longer meromorphic since $E_m(ikT_1)$ has a branch cut along the positive imaginary k-axis. This is a consequence of the power-law tail of $p_B(\Delta)$.

We therefore have to modify the contour used in section 2.1

$$\mathrm{tr}\,\mathcal{L}^t = \frac{1}{2\pi\mathrm{i}}\int_{\gamma_{\mathrm{branch}}} \mathrm{e}^{\mathrm{i}kt}\frac{Z'(k)}{Z(k)}\,\mathrm{d}k + \sum_{\alpha}\mathrm{e}^{\mathrm{i}k_\alpha t} \tag{30}$$

where γ_{branch} is given in figure 2. We now get

$$\mathrm{tr}\,\mathcal{L}^t = \Psi_{\mathrm{zeros}}(t) + \Psi_{\mathrm{tail}}(t) \tag{31}$$

with

$$\Psi_{\mathrm{tail}}(t) = \int_0^\infty \frac{1}{\pi}\mathrm{e}^{-\xi t}\,\mathrm{Re}\left(\frac{Z'(\mathrm{i}\xi+\epsilon)}{Z(\mathrm{i}\xi+\epsilon)}\right)\mathrm{d}\xi \tag{32}$$

and $\Psi_{\mathrm{zeros}}(t)$ as before. ϵ is a small positive number. The resulting trace for Model B ($m = 3$) is shown in figure 1(b). The discrete $\Psi_{\mathrm{zeros}}(t)$ is the same as in the previous model (A) since we are using the asymptotic expressions (22) and (29). It is straightforward to show that $\Psi_{\mathrm{tail}}(t) \to -1;\ t \to 0$ and $\Psi_{\mathrm{tail}}(t) \to -T_1/2t;\ t \to \infty$. The asymptotic behaviour of the trace for general $p(\Delta)$ with power-law tail is given at the end of this section.

Let us modify the first model (A) so as to have a C^1 discontinuity instead of a C^0:

$$p_C(\Delta) = \begin{cases} N & \Delta < T_1 \\ N\exp[(T_1 - \Delta)/T_2] & \Delta \geqslant T_1. \end{cases} \tag{33}$$

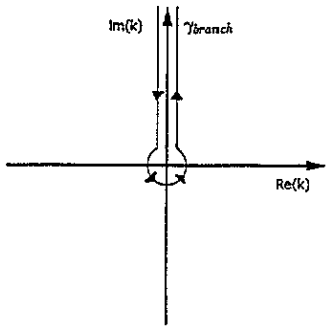

Figure 2. When $Z(k)$ has a branch cut along the positive imaginary axis the Fourier transform of the logarithmic derivative has to be integrated along γ_{branch}.

There is again a pole at $k = \mathrm{i}/T_2$. The zeros are now approximated by

$$k_n \approx \frac{1}{T_1} - \left(\pm 2\pi n + 2\mathrm{i}\ln\left(\frac{T_2}{T_1}2\pi n\right)\right) \qquad n = 1, 2, 3, \ldots . \tag{34}$$

Apart from shift a in the real direction, as compared to model A (and B), the important effect is the factor 2 in the imaginary part—the zeros lie further away from the real axis. The corresponding trace is given in figure 3.

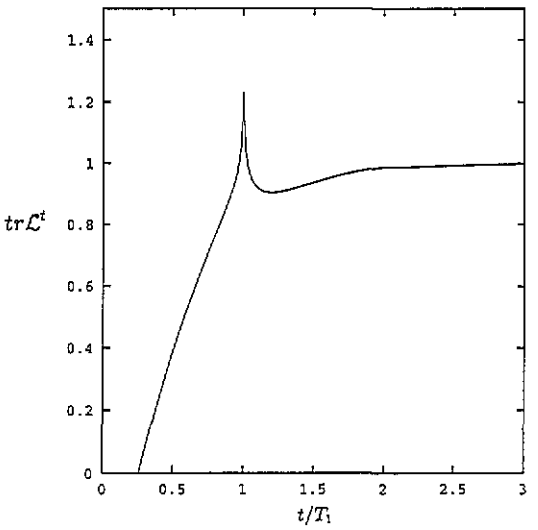

Figure 3. The trace for model C.

Finally let us demonstrate how small irregularities in $p(\Delta)$ will have a drastic effect on the spectrum. We will consider

$$p_{\mathrm{D}}(\Delta) = \begin{cases} 0 & \Delta < T \\ N(\Delta - T)\exp\left(-\dfrac{\Delta}{T}\right) & T \leqslant \Delta < 2T \\ N(\Delta - T)\exp\left(-\dfrac{\Delta}{T}\right)(1+\epsilon) & 2T \leqslant \Delta. \end{cases} \tag{35}$$

$Z_{\mathrm{D}}(k)$ has a double pole at $k = \mathrm{i}/T$. The spectrum of zeros for different perturbations, ϵ, is given in figure 4(*a*). In the low part the unperturbed spectrum is only slightly affected. The perturbation corresponds to a non-leading generation of resonances. But eventually the two generations interfere, leading to a modulation in the spectrum. For high t the higher time scale ($2T$) takes over and dominates. This result leaves us with considerable doubt on the possibility of determining the resonance spectrum from a numerically obtained probability distribution $p(\Delta)$. If there is a single dominating time scale it seems perfectly feasible [8]. But there might hide further time scales, with considerable potential impact on the spectrum. The traces for $\epsilon = 0$ and $\epsilon = 0.01$ are given in figure 4(*b*). For the unperturbed case, the trace is essentially zero when $0 < \Delta < T$. This is a remarkable conspiracy between Ψ_{zeros} and $\Psi_{\mathrm{tail}} = -2\mathrm{e}^{-t/T}$ to cancel in this way. But from a physical point of view it seems

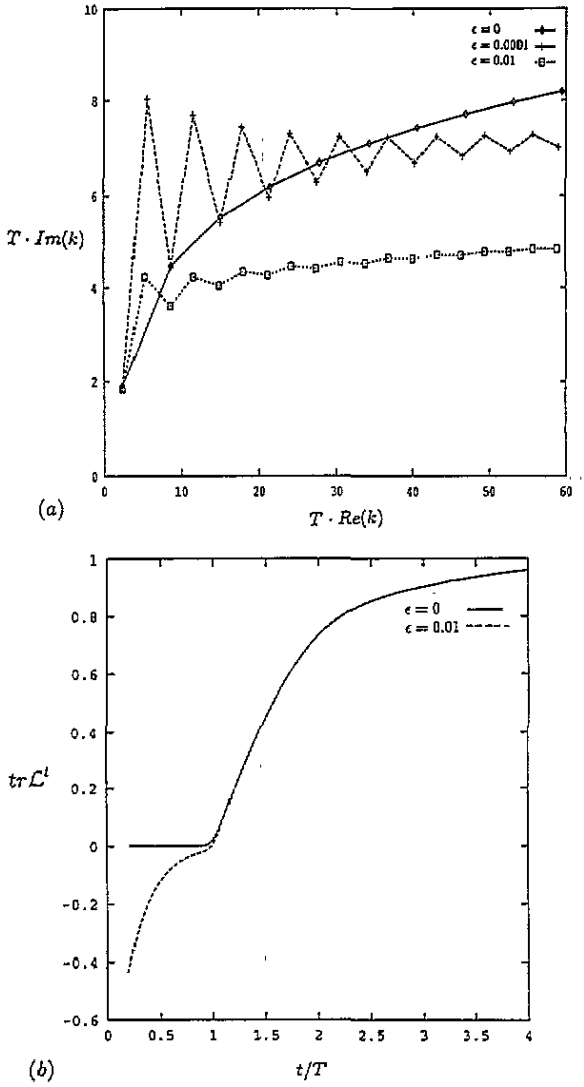

Figure 4. The spectrum (a), and the trace (b) for model D with different perturbation strengths ϵ.

sensible, cf equation (2). There is, in any system, a shortest periodic orbit, with period $T_{\min}$, such that $\mathrm{tr}\mathcal{L}^t = 0$ when $t < T_{\min}$.

When we add a perturbation, ϵ, the trace changes in two respects. First, $p_{\mathrm{D}}(\Delta)$ has a small step at $t = 2T$, which is not visible in the figure. When $0 < \Delta < T$ the trace is no longer positive definite. This is not too alarming since we have neglected $\mathrm{tr}_0(t)$ in equation (13). Moreover, the spectral sum is divergent in this region so it is questionable what confidence we should have in the results there. We have also neglected the delta function contribution from the integration over the large semicircle which of course gives a contribution to the trace for small t after smearing. For larger t we see that a small change of $p(\Delta)$ corresponds a small change in the trace, only non-leading zeros are sensitive to the perturbation.

Let us summarize our findings so far, remembering that our evidence is only heuristical and that we have assumed the exact equality $Z(k) = \hat{Z}(k)$. The zeros of the zeta function depend almost entirely on the breakpoints (i.e. different kinds of discontinuities) in the probability distribution $p(\Delta)$. Each such breakpoint introduces a time scale. When several such timescales are present the largest will dominate sufficiently high up in the spectrum, in the sense that the spacing between successive zeros in the real direction is directly related to this timescale.

The zeta function is entire only if $p(\Delta)$ decays faster than exponentially. If the decay is exponential the zeta function will have a pole on the imaginary axis. In this case the trace will approach unity exponentially fast. If $p(\Delta)$ decays as a power law there will be a logarithmic branch cut along the positive imaginary axis implying power-law convergence of the trace. It is straightforward to show that if $p(\Delta) \sim 1/\Delta^m$, the tail contribution, $\Psi_{\text{tail}}(t)$, to the trace, will behave asymptotically as

$$\Psi_{\text{tail}(t)} \to \frac{\Delta_0^m p(\Delta_0)}{(m-1)\langle\Delta\rangle} \frac{1}{t^{m-1}} \qquad t \to \infty \tag{36}$$

with $m \geqslant 3$, where $\langle\ \rangle$ denotes mean value. Δ_0 is any point in the tail of $p(\Delta)$.

4. Cycle expansions—studies of a dynamical model

In this section we will study periodic orbit expansions of the zeta function (4) for a specific dynamical system, namely the *hyperbola billiard*, i.e. a point particle elastically bouncing off the walls given by the equation

$$|xy| = 1. \tag{37}$$

An effective algorithm exists for the computation of the cycles in this system [15]. For a definition and discussion of the symbolic coding of cycles used in this paper, please consult [16]. We use units such that the particle mass $m = 1$ and we fix the energy to $E = \frac{1}{2}$, the length and time scales thus coincide. The zeta function may be factorized into the irreducible representation of the symmetry group [17], which is C_{4v} for the hyperbola billiard. We will restrict our attention to the symmetric representation A_1 containing the *trivial* zero $k_0 = 0$, [17]. This is equivalent to restricting the system to the fundamental domain [16, 17]. The periodic orbits considered in the following are periodic in this fundamental domain. They have to be retraced 1, 2 or 4 times to close on to themselves in the full system. Although we will frequently draw pictures of the periodic orbits in the full system since they are easier to visualize that way.

First we expand the m-product of (4)

$$Z(E) = \prod_p \prod_{m=0}^{\infty} \left(1 - \frac{e^{-ikT_p}}{|\Lambda_p|\Lambda_p^m}\right)^{m+1} = \prod_p \sum_{n_p=0}^{\infty} b_{n_p}(\Lambda_p)(-1)^{n_p} \frac{e^{-ikn_pT_p}}{|\Lambda_p|^{n_p}}. \tag{38}$$

Recurrence relations for the expansion coefficients b_n are derived in the appendix. If we now expand the p-product, we obtain a Dirichlet series consisting of all distinct linear combinations (pseudo-orbits) $N = [n_p]$:

$$Z(E) = \prod_N C_N e^{iT_n} \tag{39}$$

Table 1. Some simple sequences of cycles. Invariants are given for the last cycle in each sequence.

	j_{max}	$T(j_{max})$	$\Lambda(j_{max})$
210^j	3	$7.13 \equiv T_a$	19.65
21210^j	16	$18.45 \equiv T_b$	527.9
220^j	51	$27.61 \equiv T_c$	922.9
2210^j	~640	$\sim 92 \equiv T_d$	~34000
20^j	∞	—	—
110^j	∞	—	—

where we have defined the quantities

$$C_N = \Pi_p \frac{(-1)^{n_p} b_{n_p}(\Lambda_p)}{|\Lambda_p|^{n_p}} \tag{40}$$

$$T_N = \sum_p n_p T_p. \tag{41}$$

There are no obvious choices of how to order the terms, but natural choices are to order them according to (i) length of the symbol code, (ii) increasing period T_N or, (iii) decreasing *amplitudes* C_N. Our default option will be the last one. Switching between the three options will mean a complete reorganization of the sequence of the pseudo-orbits! Our default choice means that we can make no simple statements about the conditional convergence of the expansion. This will however not bother us too much. Typically, non-trivial zeros of zeta functions are positioned where the products, or series, are not even conditionally convergent, cf the Riemann zeta function, although in some lucky cases, due to alternating signs of the C_N's, they will lie in the strip of conditional convergence [18].

The idea is now to compute the partial sums (the first N_{cut} terms) and determine the zeros of the truncated expansion and study their possible convergence when N_{cut} is increased. To this end we have computed all prime orbits with eigenvalue $\Lambda_p < 2700$, and all orbits with $T < 14$, both samples containing about 10^3 orbits. To have something to cross-check our result with, we calculate the trace by means of equation (2). Of course, we have to use smearing so we replace the delta function in equation (2) with a Gaussian having width $\sigma = 0.5$. The result is given in figure 10. Due to the exponential proliferation of cycles this method soon becomes completely unrealistic as t is increased.

Our first attempt is to simply include all orbits up to the cut-off. The zeros thus found will show no tendency of convergence (the zeros drift monotonously towards the origin as N_{cut} is increased), and the trace, computed by means of the sum over zeros (again using smearing, cf equation (26)), will not show the slightest resemblance with the exact trace. *Such failures of convergence are usually due to some singularity in the zeta function.* In order to identify this we will, in some detail, study the structure of the set of cycles.

Inspired by the BER approximation we divide (somewhat ambiguously) the billiard into one chaotic part in the centre and one (almost) regular out in the arms. We can thus divide the cycles into three subsets.

1. Cycles with bounces exclusively in the chaotic region. The eignenvalues Λ are exponentially bounded with length.
2. Cycles with bounces in both regions.
3. Cycles with bounces exclusively in the regular arms.

In the following we will focus our attention on the types of cycles which dominate the expansion, with ordering chosen as above. These are the pseudo-orbits with large C_N which means that the important cycles come from set 2 and 3 above—cycles spending most of the time in the arms.

It is also convenient to distinguish between *simple* cycles, that is cycles making only one (or no) excursion into an arm, and *composed*, that is cycles making more than one such excursion. The simple cycles occur in sequences of the form $p0^j$ where the row of 0's corresponds to a number ($\sim j$) of oscillating bounces in an arm and p corresponds to the behaviour of the central region.

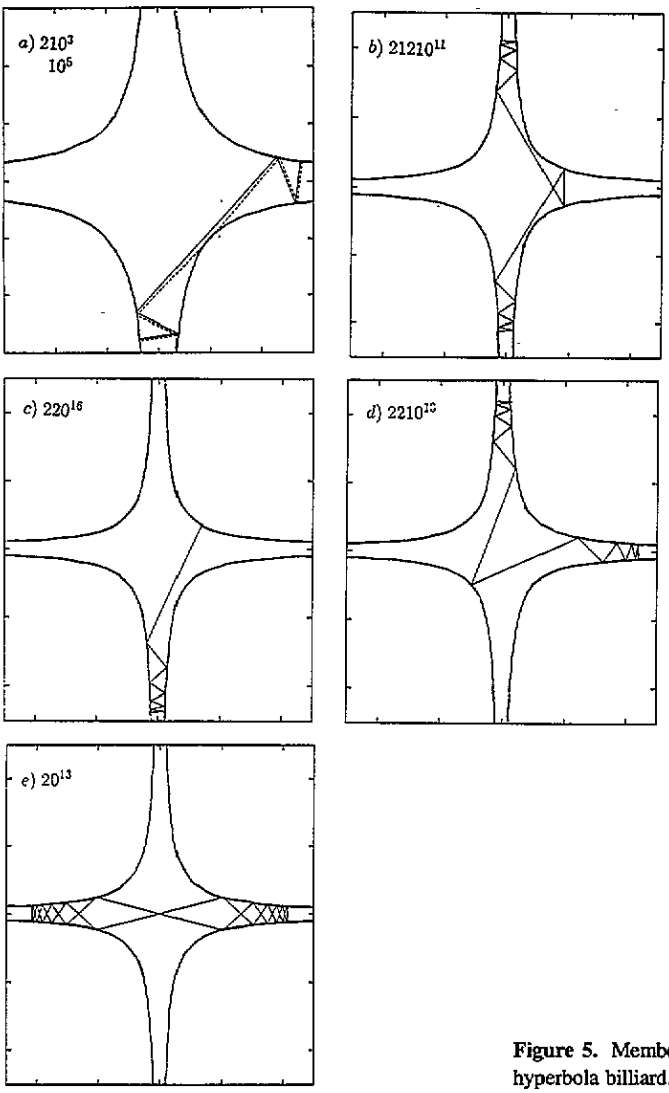

Figure 5. Members of some simple sequences in the hyperbola billiard.

Some examples of simple cycles are given in table 1 and figure 5. Cycles belonging to the sequences 20^j and 110^j make one excursion into an arm and are then injected into the opposite arm without any bouncing in the central chaotic region. These two sequences are

in fact unbounded. All other simple sequences are, we believe, finite. A cycle 210^j makes a number of oscillations in one arm, sneaks into a neighbouring arm without bouncing in the middle. This is obviously a very short sequence. A cycle in the sequence 220^j makes a number of oscillations in one arm, makes one scattering in the central region and is then injected back into the arm it came from. A cycle 2210^j makes a number of oscillations in one arm, bounces once in the central region and is then injected into a neighbouring arm.

It is obvious from figure 5 why finite families $p0^j$ are terminated at some $j = j_{\max}$. There is a section of the orbit in the central region coming closer and closer to a branch of the boundary as j is increased. When $j = j_{\max} + 1$ the orbit would need to go through this branch which it of course is not allowed to. For this reason the finite sequences are naturally organized into families where one member goes directly to the opposite branch when another member hits a branch on the way, see figure 5(a). Thus 210^j may be considered as a member of (210^j, 10^{j+3}). Other important families are (220^j, 2110^j, 1210^j, 1010^{j+1}) and (2210^j, 2010^{j+1}, 120^{j+1}, 1110^{j+2}). All members of a family terminate at the same $j = j_{\max}$, cf [16, 19]. The family member with the fewest bounces in the central region has the largest weight and the rest are of minor importance.

The class consisting of infinite simple sequences will be named $\mathcal{C}_{\inf}$ in the following and contains only 20^j and 110^j. The class of simple finite sequences is named $\mathcal{C}_{\text{fin}}$. The orbits in these classes are taken from sets (2) and (3) above, respectively. The orbits in subset (1) may be absorbed into e.g. class $\mathcal{C}_{\text{fin}}$.

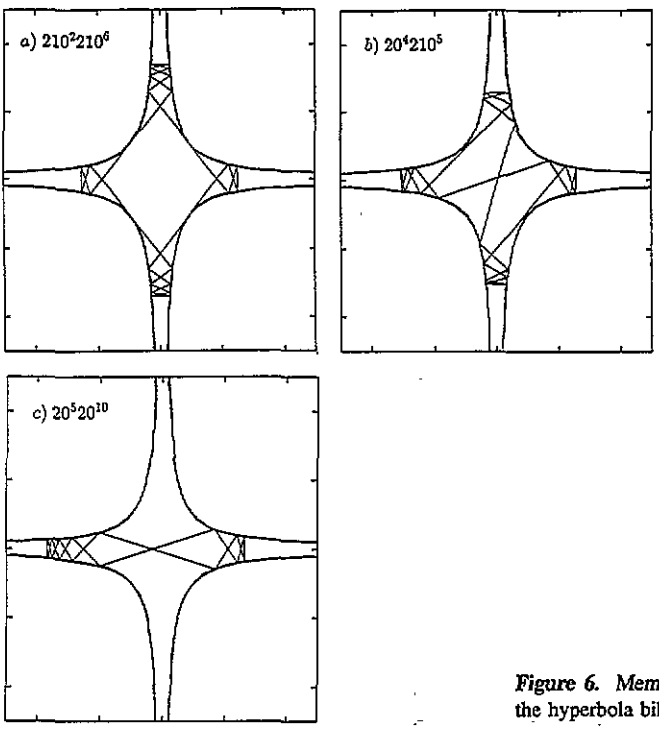

Figure 6. Members of some composed sequences in the hyperbola billiard.

Composed cycles doing two excursions into the potential arms may be written in the form $p_1 0^{j_1} p_2 0^{j_2}$. Picking the simple cycles (or rather symbol strings) $p_1 0^{j_1}$ and $p_2 0^{j_2}$ from $\mathcal{C}_{\inf}$ and/or $\mathcal{C}_{\text{fin}}$ we can construct three classes of such composed cycles: $\mathcal{C}_{\inf} * \mathcal{C}_{\inf}$,

$\mathcal{C}_{\text{fin}} * \mathcal{C}_{\text{fin}}$ and $\mathcal{C}_{\text{fin}} * \mathcal{C}_{\text{fin}}$. Generalization to higher orders are strightforward. Members of the 2-composed sequences $20^{j_1}20^{j_2}$, $20^{j_1}210^{j_2}$ and $210^{j_1}210^{j_2}$ (from the three classes respectively) are displayed in figure 6. The latter two are again finite. The allowed cycles may be represented in the j_1, j_2 plane as in figure 7.

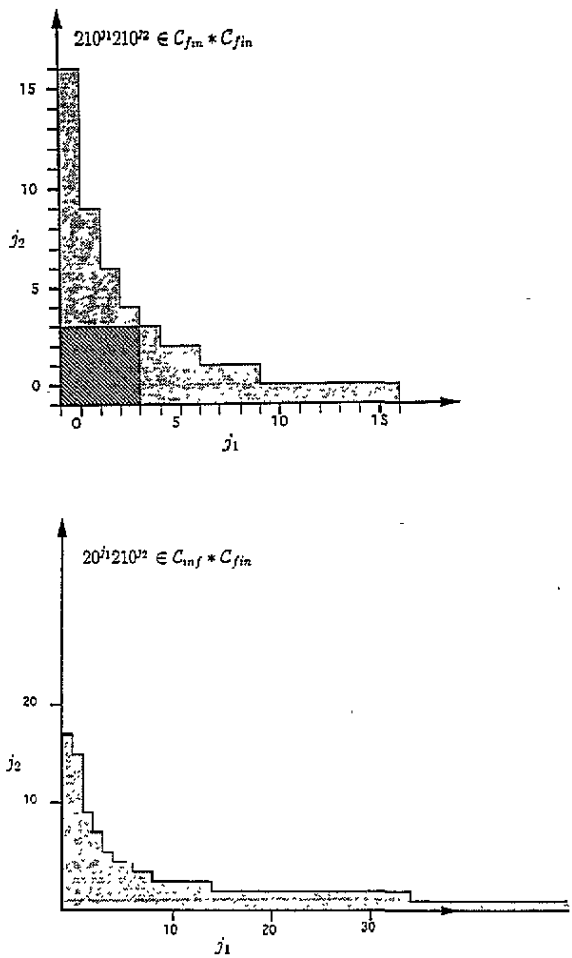

Figure 7. Graphical representation of the allowed cycles in some composed sequences.

The region of allowed cycles is quite different from the class $\mathcal{C}_{\text{inf}} * \mathcal{C}_{\text{inf}}$. Take for example the $20^{j_1}20^{j_2}$ sequence. In the adiabatic approximation one can show that, in the limit $j_1 \gg 1$ and $j_2 \gg 1$, the allowed cycles lie in the infinite region.

$$\frac{j_1}{a} < j_2 < a \cdot j_1 \tag{42}$$

where $a \approx 1158$.

Of course, the division between simple and composed cycles is again somewhat ambiguous; e.g. should 21210^j be considered as simple or to belong to the composed sequence $210_1^j 210_2^j$, cf figure 5(*b*) and 6(*a*)?

Let us now discuss the contributions of the different sequences to the expansion of the zeta function.

We begin with the class $\mathcal{C}_{\text{inf}}$. For large j it was shown in [20] that the periods and the stability eigenvalues for the 20^j and 110^j sequences are:

$$T_j \approx \sqrt{4\pi(j+1)} \qquad \Lambda_j \approx c(j+1) \qquad j = 1, 2, \ldots, \infty \tag{43}$$

where $c = 117/4$ for 20^j. The corresponding factor for 110^j is much bigger. We suspect these infinite sequences to be the main cause of our divergence problem. Before following this track we discuss the finite sequences.

A finite simple sequence $p0^j$ will have invariants depending on j similarly to the infinite ones above, but with j terminating at some $j_{\max}$ (see table 1). The slope of Λ_j versus j will depend on the behaviour in the central region and seems to be exponentially bounded with the number of bounces there. Each finite sequence naturally introduces a time scale given by the period of the last orbit, some of these timescales are named in the table. The trace, figure 10, will obviously show a sudden decrease; cf equation (2) at any such time scale. In figure 10 they are rather recognized as smooth peaks due to smearing. This (infinite) set of timescales are essential for the problem and will be reflected by the zeros of the zeta function.

The cross-terms between simple orbits are naturally discussed on the same footing as the composed sequences. There is a potential possibility of shadowing, that is, the term due to orbit $p_1 0^{j_1} p_2 0^{j_2}$ is compensated by the pseudo-orbit consisting of $p_1 0^{j_1}$ and $p_2 0^{j_2}$. This can however only be partly realized due to the finiteness (*pruning*) of the sequences. The double hatched area in figure 7(*a*) shows where there exist compensating cross-terms. However, these terms are sparse in the expansion, and may in some sense be considered as corrections, cf the *curvature corrections* in [11]. The orbits along the boundary of the allowed region (cf figure 7) also introduce timescales.

We suspected the class $\mathcal{C}_{\text{inf}}$ to be the main cause of our problem. We will now attempt a factorization

$$Z(k) = Z_1(k) \cdot Z_2(k) \tag{44}$$

where, in the first factor, we only include cycles $p \in \mathcal{C}_{\text{inf}}$ and in the second we include the rest $p \in \mathcal{C}_{\text{tot}} - \mathcal{C}_{\text{inf}}$. The first factor is approximately

$$Z_1(k) \approx 1 - \frac{1}{c} \sum_{j=1}^{\infty} \frac{e^{-i\sqrt{4\pi j}k}}{j}. \tag{45}$$

Cross-terms are sparse in the series, so we have omitted them. It is straightforward to see that the function defined by this sum have a logarithmic branch cut along the positive imaginary axis.

Our hope is now that the eigenvalues are given by the zeros of $Z_2(k)$, which is expanded as before. We now seem to obtain a well defined spectrum where when $N_{\text{cut}} > 180$ see figure 8! However, we do not find much improvement when N_{cut} is increased further. It is thus obvious that the zeta function needs further regularization. The convergence of the trivial zero k_0 is plotted in figure 9. The convergence is extremely slow which reflects the fact that the zero sits on a singularity (branch cut) which has not been completely removed.

We obviously need some support for our claim that the obtained spectrum is indeed close to the exact one. To that end we compute the trace by means of the sum over zeros

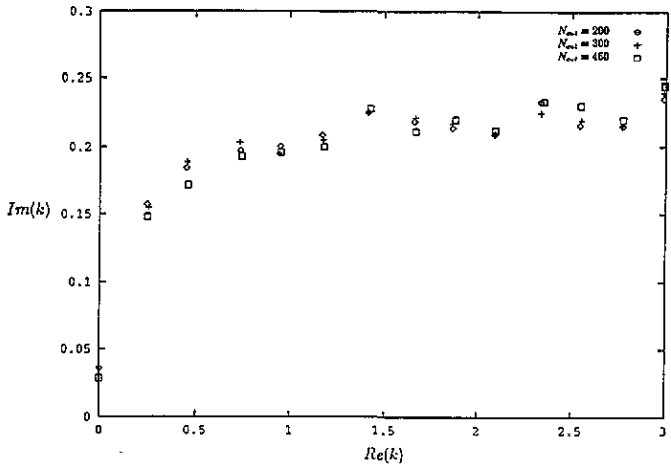

Figure 8. Spectrum of the hyperbola billiard for various numbers of pseudo-orbits N_{cut}.

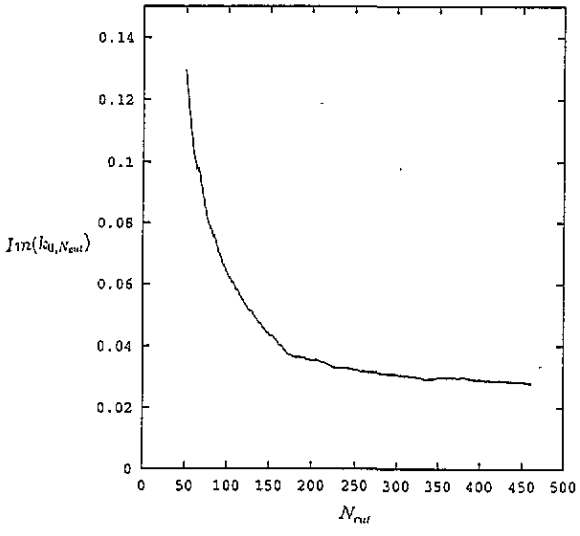

Figure 9. Location of the zero k_0 as a function of N_{cut}.

$\Psi_{\mathrm{zeros}}(t) = 1 + \sum_n \mathrm{e}^{\mathrm{i}k_n t}$ and compare with the exact result due to equation (2). Again we use Gaussian smearing, which is unavoidable since we only have a finite sample of zeros of $Z(k)$. The result is plotted in figure 10. We see that the curves closely resemble each other on the small scale structure.

Let us first study the structure of the spectrum (cf figure 8). We recognize several features from the spectra in section 3. The imaginary part of the zeros increase slower than logarithmically with the real parts (cf model D in section 3). We also recognize a modulation of the spectrum. These features indicate that several time scales are involved. The real parts of the zeros are more or less equally spaced. The mean spacing corresponds to a time scale $T \approx 27.8$ which is much longer than the shortest periodic orbit of the system, $T_{\mathrm{min}} = 2$. It is indeed close to the timescale $T_c \approx 27.61$ associated with the sequence 220^j

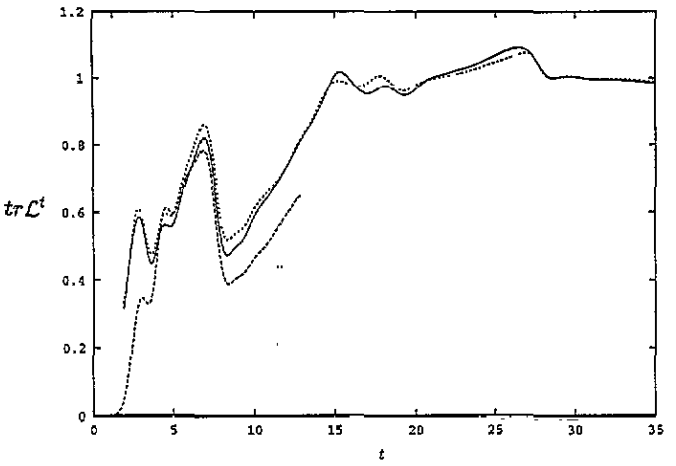

Figure 10. The trace for the hyperbola billiard using direct summation (equation (2)) (long dashed), and as a sum over eigenvalues, with $N_{\text{cut}} = 200$ (short dashed), and $N_{\text{cut}} = 460$ (full line).

which dominates the expansion of Z_2 for the first 180 terms. Clearly, using ordering option (ii) we would need all cycles with $T_p \leqslant T_c$ in order to resolve the spectrum. This would mean $\sim 10^6$ cycles. With the ordering option chosen we have managed to obtain a good approximation to the spectrum using a thousand times fewer orbits!

In figure 10 we see that the exact trace and the sum Ψ_{zeros} differ by a slowly varying function. The immediate suggestion to explain this discrepancy is that there is another contribution to the trace from a pole or a branch cut, cf Ψ_{tail}. The latter possibility is suggested by the function $Z_1(k)$ having a branch cut. However, we do not yet claim that $Z_2(k)$, as defined above, is entire. We cannot expect the branch cut to be factored out that easily. This means that we cannot compute this extra contribution only from Z_1.

The problems encountered so far could be somewhat enlightened by explicit knowledge of the probability distribution $p(\Delta)$ for the billiard since we expect there to be a close relationship between its Fourier transform and the zeta function. This is easily obtained by simulating the system. It is thus essential that we take advantage of the adiabatic invariance in the arms, cf [20]. There is no sharp borderline between the chaotic and regular part of the billiard. We make an arbitrary division at some $x = x_{\text{div}}$ (remember the system is defined on the fundamental domain $y > 0, y < x$). The result is given in figure 11. The histogram is based on 10^6 visits in the arm and the borderline is set to $x_{\text{div}} = 4$.

We recognize the time scales as introduced above and defined in the table, as underlying the structure of $p(\Delta)$. For small $\Delta < 15$ the result is sensitive to the exact location of the borderline. But the rest of $p(\Delta)$ is rather insensitive to it.

The curve exhibit a peak around $\Delta \approx T_b$. Among the *important* composed sequences $210^{j_1}210^{j_2}$ and $20^{j_1}210^{j_2}$ (with $j_1 \neq 0$) all cycles have $T < T_c$, and indeed their periods are distributed around the peak of $p(\Delta)$.

When $T_c < \Delta < T_d$, $p(\Delta)$ is decreasing exponentially to a high degree of accuracy. In the region of exponential decay there seems to be a gap, with no pronounced timescales (as defined by means of finite sequences).

When $\Delta > T_d$, the curve slowly begins to deviate from the exponential. Relevant sequences for this tail are e.g. $20^{j_1}20^{j_2}$—the sequence 2020^j terminates at $j \approx 990, T \approx 116$.

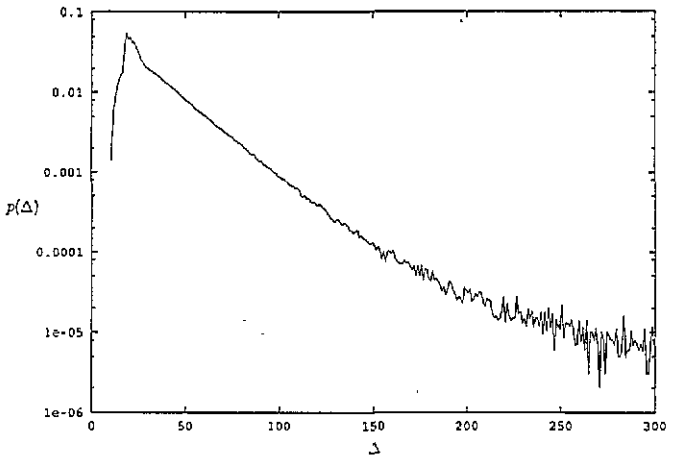

Figure 11. $p(\Delta)$ in the hyperbola billiard obtained by numerical simulation.

It would be highly desirable to know the asymptotic form of $p(\Delta)$; if possible we could be able to estimate the branch cut contribution $\Psi_{\text{tail}}(t)$. However, the crossover from exponential decay to something else (power law?) warns us that $p(\Delta)$ is not easily extrapolated. There may be hiding more surprises higher up. Estimating the tail behaviour by analytical means would require a detailed understanding of how the almost integrable arms are coupled through the chaotic central region. The problem lies in the very long laminar phases (large Δ) which have segments of the trajectory coming from one arm and injected directly into the opposite without bouncing in the chaotic part (in the simulation we require at least one central bounce to consider the laminar phase as terminated). From a cycling point of view the classes C_{inf}, $C_{\text{inf}} * C_{\text{inf}}$ etc are central for the description of these trajectories. Excluding C_{inf} as a first step in the regularization, as we did, seems quite reasonable. However, to proceed the regularization scheme further will require entirely new ideas. Such a procedure would probably reveal more singularities.

In the calculation of the spectra above we concluded that the time scale T_c is in some sense dominant. An explanation of this is offered by the shape of $p(\Delta)$. T_c is the last timescale (breakpoint) before the exponential part of $p(\Delta)$. We concluded in section 3 that such a behaviour of $p(\Delta)$ would lead to a mean spacing corresponding to T_c, at least in the lower part of the spectrum.

We have been content with showing that the different timescales may be found in $p(\Delta)$ and have not been tempted to utilize the histogram of $p(\Delta)$ to calculate a spectrum. This is not feasible from such a coarse histogram. Moreover, the fine structure is blurred by the ambiguity of the borderline between the chaotic and the laminar regions.

Although this section has ended in some frustration we summarize our main findings: We have computed several isolated zeros of the zeta function for the hyperbola billiard. We have also presented evidence for a branch cut in the zeta function implying slower-than-exponential decay of the trace. The evidence is threefold. First, the presence of the branch cut in the function Z_1 defined in equation (44). Secondly, the slower-than-exponential decay of the function $p(\Delta)$ in figure 11. Thirdly, the discrepancy between the curves in figure 10 obtained from exact summation of the trace and as a sum over discrete zeros. Finally we have identified a dominant time scale which is much longer than the shortest periodic orbit of the system. Time scales are introduced into the system by the termination of finite sequences of periodic orbits.

5. Semiclassical implications

A very interesting application of the *trace* concerns correlations in quantum spectra. The reason for this coupling is the close resemblance between the classical zeta function (4) and the semiclassical one [21]

$$Z_{sc}(E) = \prod_p \prod_{m=0}^{\infty} \left(1 - \frac{e^{iS_p(E) - \mu_p(\pi/2)}}{|\Lambda_p|^{1/2}\Lambda_p^m}\right). \tag{46}$$

The μ_p's are the Maslov indices and S_p are the action integrals which for homogeneous potentials, such as billiards, are proportional to the periods T_p times some power of the energy E. The zeros of this object are (in the semiclassical limit) the quantum eigenvalues. The spectral density, as given by the logarithmic derivative of Z_{sc}, yields the Gutzwiller trace formula [22].

One such interesting correlation measure is the spectral rigidity $\Delta_3(L)$. It is defined as follows. Given the quantum spectra $\{E_i\}$, consider the spectral staircase function $N(E) = \sum_i \theta(E - E_i)$. Now, make the best fit, by means of the least square method, by a linear function over L mean level spacings. Calculate the square deviation between $N(E)$ and this linear function, average this quantity over an energy interval ΔE which contains many levels but is semiclassically small (ΔE is smaller than the energy scale given by the shortest periodic orbit in the system), and you end up with the function $\Delta_3(L)$. Under the assumption that the trace, $\mathrm{tr}\,\mathcal{L}^t$, is exactly one when $t > T_{min}$ Berry [23] showed that $\Delta_3(L)$ is consistent with GOE for a range $0 < L < L_{max}$ where L_{max} corresponds to T_{min}, if the system is chaotic and time reversible. But for bound chaotic systems we have realized that the trace may be significantly different from one up to a time scale much bigger than T_{min}. This means that there is a region in $L < L_{max}$ where $\Delta_3(L)$ *cannot* exhibit universal behaviour and where we *can* perform semiclassical calculations. This is really what *quantum chaology is about, to relate the quantum behaviour to the classical* by semiclassical methods. Indeed, such departure from universality for $L < L_{max}$ has been observed in a number of numerical calculations [24–26]. Moreover, if there is a contribution from a branch cut of the zeta function we expect the trace $\mathrm{tr}\mathcal{L}^t$ not to approach unity exponentially but rather as a power law. This extends further the dynamical interesting region in L. Indeed one can show that if the trace goes asymptotically as $\mathrm{tr}\,\mathcal{L}^t \to 1 - c/t$ the universal (GOE) result can only be achieved in the deep asymptotic limit $E \to \infty$.

Time scales in connection with the spectral rigidity have been discussed in [25].

We have seen that the trace for the hyperbola billiard is closer to 0.5 than 1.0, for a considerable range in t. This means that the $\Delta_3(L)$ should be closer to the GUE result than to the GOE (which would be appropriate since the system is time reversible); this is exactly what is observed in a quantum mechanical calculation [26].

A lot of the recent work in the area of quantum chaology has been occupied with the problem of relating *individual* eigenstates to the periodic orbits. Due to the exponential proliferation of cycles this cannot be pursued very high up in the spectrum. This problem is in itself very interesting. But, if we want to use semiclassical methods to investigate the transition from classical to quantum mechanics, that is, if we are interested in (asymptotically) high states, then we are bound to understand the asymptotics of the set of periodic orbits and this is, as we have seen, related to the tail of the probability distribution $p(\Delta)$. The problem of exploring the asymptotics of the set of cycles by explicitly computing them is well exemplified in [27].

6. Concluding remarks

In this paper we have discussed relations between periodic orbits, the resonance spectrum and the dynamical behaviour of a system. We have suggested a close relationship between the classical zeta function $Z(k)$ and the corresponding function $\hat{Z}(k)$ as obtained from the BER approximation. We have not pursued this relation very far for the hyperbola billiard. This system is peculiar having infinite phase-space volume so that the derivation in section 2.2 becomes dubious. To study these ideas in detail will require much more theoretical work as well as numerical studies of a range of systems. Ergodic billiards calling to be investigated in this respect are e.g. the Sinai billiard and the closed three disk billiard. For the Sinai billiard it is straightforward to show that the function $p(\Delta)$ should decay as $1/\Delta^3$ suggesting that the trace behaves asymptotically behaves as $\mathrm{tr}\mathcal{L}^t \to 1 - \mathrm{const}/t$.

For the case of the hyperbola billiard we observed that the relevant time scale was much larger than the period of the shortest cycle. The dominant time scale for the Sinai billiard should be the mean free path between the disks bounces which is also much longer than the shortest cycle, for small disk radii.

There is of course a more straightforward method to determine correlation spectra. This is to numerically simulate the system, compute the correlation function for some physical observable(s), make a Fourier transform and then locate its poles. This is feasible for discrete time systems (maps) since power series are easily analytically continued by standard Padé techniques. But continuous time system (flows), as we have considered in this paper, would make that method much more tedious.

The BER approximation offers us, in principle, a way to deduce the spectrum from knowledge of $p(\Delta)$ which is often easy to obtain, numerically or by other means. However, we have argued that it may be hard to determine the non-leading zeros from a numerically obtained histogram, and often periodic orbit theory seems to be superior. But an interesting question is whether cycle expansions can be improved by knowledge of the leading singularities, as obtained from the tail of $p(\Delta)$. The optimal way to attack the hard problem of bound chaotic systems may perhaps be found through crossfertilization of present techniques.

It is our hope that this paper provides some ideas for work along these lines.

Acknowledgments

Finally I would like to thank Predrag Cvitanović, Hans Henrik Rugh and Viviane Baladi for valuable discussions. This work was supported by the Swedish Natural Science Research Council (NFR) under contract no. F-FU 06420-303.

Appendix

We now demonstrate how to obtain a recurrence relation for the coefficients of the expansion of

$$\prod_{k=0}^{\infty}\left(1+\frac{t}{\Lambda^k}\right)^{k+1} = \sum_{n=0}^{\infty} b_n(\Lambda)t^n. \tag{47}$$

Consider first the simpler problem of expanding the Euler product

$$\prod_{k=0}^{\infty}\left(1+\frac{t}{\Lambda^k}\right)=\sum_{n=0}^{\infty}a_n(\Lambda)t^n!. \tag{48}$$

We extract the first factor

$$\prod_{k=0}^{\infty}\left(1+\frac{t}{\Lambda^k}\right)=(1+t)\prod_{k=1}^{\infty}\left(1+\frac{t}{\Lambda^k}\right)=(1+t)\sum_{n=0}^{\infty}a_n(\Lambda)(t/\Lambda)^n \tag{49}$$

and obtain the recurrence formula

$$a_n=\frac{\Lambda^{1-n}}{1-\Lambda^{-n}}a_{n-1}\qquad a_0=1 \tag{50}$$

which can be solved exactly

$$a_n=\frac{\Lambda^{-n(n-1)/2}}{\prod_{k=1}^{n}(1-\Lambda^{-k})}. \tag{51}$$

We now use the same technique for equation (47)

$$\begin{aligned}\prod_{k=0}^{\infty}\left(1+\frac{t}{\Lambda^k}\right)^{k+1}&=\prod_{k=0}^{\infty}\left(1+\frac{t}{\Lambda^k}\right)\cdot\prod_{k=1}^{\infty}\left(1+\frac{t}{\Lambda^k}\right)^{k}\\&=\left(\sum_{n=1}^{\infty}a_n(\Lambda)t^n\right)\left(\sum_{n=1}^{\infty}b_n(\Lambda)(t/\Lambda)^n\right)\end{aligned} \tag{52}$$

leading to the recurrence relation

$$b_n=\frac{1}{1-\Lambda^{-n}}\sum_{l=0}^{n-1}a_{n-l}b_l\Lambda^{-l}\qquad b_0=1. \tag{53}$$

References

[1] Pollicott M 1986 *Inv. Math.* **85** 147
[2] Ruelle D 1986 *J. Stat. Phys.* **44** 281
[3] Ruelle D 1986 *J. Diff. Geom.* **25** 99, 117
[4] Rugh H H 1992 *Nonlinearity* **5** 1237
[5] Ruelle D 1983 *C. R. Acad. Sci. Paris Sér. I* **296** 191
[6] Pollicott M 1984 *Ergod. Th. Dynam. Sys.* **4** 135
[7] Dahlqvist P and Russberg G 1990 *Phys. Rev. Lett.* **65** 2837
[8] Baladi V, Eckmann J P and Ruelle D 1989 *Nonlinearity* **2** 119
[9] Hannay J H and Ozorio de Almeida A M 1984 *J. Phys. A: Math. Gen.* **17** 3429
[10] Cvitanović P and Eckhardt B 1991 *J. Phys. A: Math. Gen.* **24** L237
[11] Artuso R, Aurell E and Cvitanović P 1990 *Nonlinearity* **3** 325, 361
[12] Cvitanović P and Eckhardt B 1989 *Phys. Rev. Lett.* **63** 823
[13] Eckhardt B and Russberg G 1993 *Phys. Rev.* E **47** 1578

[14] Abramovitz M and Stegun I A 1964 *Handbook of Mathematical Functions* (Washington: National Bureau of Standards)
[15] Sieber M and Steiner F 1990 *Physica* D **44** 248
[16] Dahlqvist P and Russberg G 1991 *J. Phys. A: Math. Gen.* **24** 4763
[17] Cvitanović P and Eckhardt B 1993 *Nonlinearity* **6** 277
[18] Aurich R, Bolte J, Matthies C, Sieber M and Steiner F 1993 *Physica* D **63** 71
[19] Hansen K 1991 *Chaos* **2** 71
[20] Dahlqvist P 1992 *J. Phys. A: Math. Gen.* **25** 6265
[21] Voros A 1988 *J. Phys. A: Math. Gen.* **21** 685
[22] Gutzwiller M C 1990 *Chaos in Classical and Quantum Mechanics* (New York: Springer)
[23] Berry M V 1985 *Proc. R. Soc* A **400** 229
[24] Wintgen D, Marxer H and Briggs J S 1988 *Phys. Rev. Lett.* **61** 1803
[25] Arve P 1991 *Phys. Rev.* A **44** 6920
[26] Sieber M 1991 *The Hyperbola Billiard: A model for Semiclassical Quantization of Chaotic Systems, Thesis,* Fachbereichs Physik der Universität Hamburg
[27] Argaman N, Doron E, Keating J, Kitaev A, Sieber M and Smilansky U 1992 *Correlations in the Actions of Periodic orbits Derived from Quantum Chaos, Preprint* WIS-92/73/Sept-PH (Israel: Rehovot)